Out-of-time-ordered correlator in the quantum bakers map and truncated unitary matrices

Arul Lakshminarayan
Department of Physics, Indian Institute of Technology Madras, Chennai 600036, India

(Received 1 November 2018; published 2 January 2019)

The out-of-time-ordered correlator (OTOC) is a measure of quantum chaos that is being vigorously investigated. Analytically accessible simple models that have long been studied in other contexts could provide insights into such measures. This paper investigates the OTOC in the quantum bakers map which is the quantum version of a simple and exactly solvable model of deterministic chaos that caricatures the action of kneading dough. Exact solutions based on the semiquantum approximation are derived that tracks very well the correlators until the Ehrenfest time. The growth occurs, surprisingly, at the exponential rate of the classical Lyapunov exponent which is half of that expected semiclassically. This exponential growth is modulated by slowly changing coefficients. Beyond this time, saturation occurs at a value close to that of random matrices. Using projectors for observables naturally leads to truncations of the unitary time-t propagator and the growth of their singular values is shown to be intimately related to the growth of the out-of-time-ordered correlators.

DOI: 10.1103/PhysRevE.99.012201

I. INTRODUCTION

Quantum mechanics of low-dimensional systems with a deterministically chaotic classical limit have attracted steady attention since the late 1970s, and textbooks such as [1–4] chronicle a variety of these studies. These pose significant challenges and have given us various insights, including semiclassical periodic orbit theory and the relevance of random matrix ensembles for even one-particle systems whose classical limit is chaotic and surveys collected in [5] form an excellent introduction. A resurgence of interest in quantum chaotic or nonintegrable systems has occurred around the related themes of scrambling and out-of-time-ordered correlators or OTOCs [6–13]. The OTOC, as commonly defined, is connected to the development of noncommutativity of initially commuting operators [14] and therefore this forms a convenient starting point. In the context of many-body systems they capture how initially localized information spreads and is related to the Lieb-Robinson bound for commutator growth in systems with a finite range of interactions [15,16].

In the recent past, it has been used in the study of quantum field theories and black holes, which are said to be nature's fastest scramblers as they saturate a conjectured upper-bound on chaos [14,16,17]. A, by now standard, qualitative motivation for relating commutators with chaos is that $-\langle[\hat{q}(t),\hat{q}(0)]^2\rangle \sim \hbar^2\{q(t),q(0)\}^2 = \hbar^2[\partial q(t)/\partial p(0)]^2 \sim \hbar^2 e^{2\lambda t}$, where the semiclassical connection with Poisson brackets is used and further in the last step a chaotic evolution with a Lyapunov exponent of λ is assumed. Thus the growth of the commutator is a quantum measure of instability, and the Lyapunov exponent growth is expected in a time regime that is between a diffusion time scale t_d and the Ehrenfest time scale t_{EF} at which quantum-classical correspondence, if any, breaks down. The growth of the commutator being a purely quantum measure can be used in systems such as spin chains which have no apparent classical limits and is a dynamical measure of the system's complexity.

Simple models from classical dynamical systems have played an important role in the study of quantum chaos. These include quantum maps [18,19], which are Floquet systems or quantizations of finite canonical transformations which have also been invoked in recent studies of OTOCs. For example, the standard map or kicked rotor has been studied in [6] while the quantum cat map and its perturbed versions have been studied in the context of operator spreading and OTOCs [9,13]. The classical cat map, introduced by Arnold and Avez [20], is a smooth linear area-preserving map of the two-torus into itself. Its quantization [21] possesses nongeneric features such as exact periodicity in time, which is overcome by smooth perturbations on it but renders it analytically intractable. The classical bakers map, introduced by Hopf [22] is a discontinuous linear transformation of the phase space, in the form of a square, into itself that is a caricature of the actions involved in kneading dough that leads to a uniform mixture, an essential prerequisite for good pastry. It is an exactly solvable and deterministic model of chaos [23,24], and yet is strongly stochastic in the sense that it is isomorphic to a Bernoulli process, in other words it is as random as a coin toss [25] and has been described as the "harmonic oscillator of chaos."

The quantization of the bakers map, which treats the phase space square as a torus, has been studied in many different flavors since the original quantization by Balazs and Voros [26,27]. The quantum map consists of discrete Fourier transforms on appropriate spaces and is hence a simple N-dimensional unitary matrix B which has also been implemented in an NMR experiment [28,29]. It can be considered, when the Hilbert space dimension $N = 2^L$, as dynamics of L qubits with nonlocal interactions and entanglement in these qubits have also been studied [30]. However, despite its simplicity, it has not yet been solved analytically, say for its eigenspectra which have a close resemblance to those of random matrix ensembles [31]. In this sense it is arguably less valuable than its classical counterpart. Nevertheless there

are some simplifications in the sense that the powers of the classical map can be independently quantized and a simpler operator results that is not the powers of the quantum map itself [32,33]. This "delayed quantization" has been called semiquantum and provides a valuable approximation B_t for the time evolved propagator (the powers of the matrix B^t). For example this is the starting point for a semiclassical periodic orbit quantization of the bakers map [34].

The semiquantum approximation is used below to evaluate analytically the OTOC for the quantum bakers map. By construction the semiquantum approximation is valid only until the Ehrenfest time and therefore the OTOC can be explicitly found in its Lyapunov regime. The analytical results reveal a surprisingly complex situation with the rate reaching the classical Lyapunov exponent λ (and *not twice* this) at late times. The origin for this could be from the dynamics being nonsmooth, giving rise to "diffraction" effects. It is known [35] that sufficiently localized operators are needed for quantum classical correspondence to exist, localized enough to not suffer the discontinuities within the Ehrenfest time. The other is also that the operators themselves need not have smooth classical symbols with which to compute their Poisson or Moyal brackets. For the bakers map it is the former property that results in this rate being different from 2λ and closer to λ, as we see this also for operators with smooth classical limits. However in this work, we consider for analytical purposes phase space projection operators whose classical limits are evidently characteristic functions on phase space. This allows for the OTOC to be written exclusively based on a truncation of the unitary propagator B^t to a nonunitary operator. That the spectrum and singular values of such truncations carry information about scrambling is a general feature.

Consider the noncommutativity of Hermitian operators $A(0)$ and $A(t)$ as given by

$$f(t) = -\tfrac{1}{2}\mathrm{Tr}[A(t),\ A(0)]^2 = f_2(t) - f_4(t),$$
$$f_2(t) = \mathrm{Tr}[A(t)^2 A(0)^2], \quad f_4(t) = \mathrm{Tr}[A(t)A(0)A(t)A(0)], \tag{1}$$

where $A(t) = U^{-t}A(0)U^t$ is the operator evolved to time t by the dynamics of the propagator U^t. The term $f_2(t)$ is a two-point correlation, while $f_4(t)$ is a four-point OTOC. Let the operator $A(0)$ be a projector

$$P(0) = \sum_{j=j_{\min}}^{j_{\max}} |j\rangle\langle j|, \tag{2}$$

where $\{|j\rangle,\ 0 \leqslant j \leqslant N-1\}$ forms a complete orthonormal basis. Let $J = [j_{\min}, j_{\max}]$ be the range of the projector, and let the complementary range be $\overline{J} = [0, j_{\min}-1] \cup [j_{\max}+1, N-1]$. We will also use the same letter J to denote the dimensionality $j_{\max} - j_{\min} + 1$ of the projector space. It follows that

$$f_2(t) = \mathrm{Tr}[P(t)P(0)] = \mathrm{Tr}(\tilde{U}^{t\dagger}\tilde{U}^t) = \|\tilde{U}^t\|^2, \tag{3}$$

where $P(0)U^tP(0) = \tilde{U}^t$ is a J-dimensional truncation of U^t in the basis $\{|j\rangle\}$ and the norm is Euclidean.

Such correlations have been previously studied for a variety of "interacting" bakers maps that are isomorphic to Markov chains in [36]. These quantized maps are studied as models of relaxation in classical mixing systems [37]. In general if g and h are two functions on a phase space, then $\langle h_t g\rangle - \langle h_t\rangle\langle g\rangle$ (where h_t is the time-evolved function and $\langle\cdot\rangle$ denotes phase space averaging) decay exponentially at the rates determined by the Ruelle-Pollicott resonances [38]. The change in the two-point correlator is rapid in comparison with the OTOC and is essentially governed in the classical limit by these resonances that lead to mixing. Beyond the time scales set by these, the noncommutativity grows due to the decay of the OTOC. This is the process we are interested in, but we will study the noncommutativity $f(t)$ which includes both these contributions and sometimes loosely refer to it as the OTOC itself.

The OTOC has the following simplifications:

$$f_4(t) = \sum_{j,j'\in J} |\langle j|P(t)|j'\rangle|^2 = \mathrm{Tr}(\tilde{U}^{t\dagger}\tilde{U}^t)^2 = \|\tilde{U}^{t\dagger}\tilde{U}^t\|^2. \tag{4}$$

Thus if the eigenvalues of $\tilde{U}^{t\dagger}\tilde{U}^t$, or equivalently (square of) the singular values of $\tilde{U}^t$, are $\mu_i(t)$, then these completely determine the $f_2(t)$ as well as $f_4(t)$. Their difference $f(t)$ is then

$$f(t) = \sum_{j\in J}\sum_{j'\in\overline{J}} |\langle j|P(t)|j'\rangle|^2 = \sum_{i=1}^{J} \mu_i(t)[1-\mu_i(t)]. \tag{5}$$

Truncated unitary matrices, especially from random matrix ensembles, have been studied vigorously since the pioneering work of Zyczkowski and Sommers [39] and find applications in many contexts such as chaotic scattering, where truncations of S matrices arise [40,41], open quantum systems [42], and tunneling studies [43]. Note that $0 \leqslant \mu_i(t) \leqslant 1$ and $f(t) \leqslant J/4$. The growth in norm of truncations of powers of unitary matrices are naturally related to the OTOC, an observation that may provide more insights. Apart from the singular values $\mu_i(t)$ of $\tilde{U}^t$, their complex eigenvalues also provide a characterization of the dynamics that reflects the growth of the OTOC as will be seen in the example of the bakers map.

II. PRELIMINARIES OF THE BAKERS MAP

This section is to provide an introduction (to nonbakers) of well-known facts of the bakers map, both classical and quantal.

A. Classical map

The classical bakers map is given by the transformation of $(q, p) \in [0, 1) \times [0, 1)$ to itself and is given by

$$\mathcal{T}(q, p) = (q', p') = (2q(\mathrm{mod}\ 1), (p + [2q])/2). \tag{6}$$

It is piecewise linear with a discontinuity at $q = 1/2$, and if the square is treated as a torus it is discontinuous at $q = 0$ as well. The action on the unit square is illustrated in Fig. 1, where the stretching by a factor of 2 along the q direction and compression along p is illustrated. The left vertical half L gets mapped into the bottom horizontal half B. In this action the q suffers the "doubling map" $q \mapsto 2q$ (mod 1) and the dynamics in terms of binary representation is one of the left shift [23,24]. The momentum ensures that the shifted

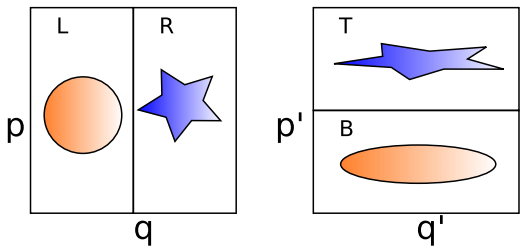

FIG. 1. The bakers map action on the unit square on the left takes it to the right, by stretching the left half L by a factor of 2 along q and compressing by a factor $1/2$ along p so that it becomes the bottom half B. The transformation from the right half R to the top half T is similar. Repeating this action constitutes a highly efficient mixing protocol and a solvable textbook example of deterministic chaos.

bits are not lost. If $q = 0.a_0a_1a_2\ldots$ and $p = 0.a_{-1}a_{-2}\ldots$ are the respective binary representations ($a_i \in \{0, 1\}$), then $q' = 0.a_1a_2a_3\ldots$ and $p' = 0.a_0a_{-1}a_{-2}\ldots$. Thus this left-shift iterated is the bakers map action that lays bare the heart of deterministic chaos. In particular the Lyapunov exponent is $\ln 2$, all its orbits are hyperbolic (unstable), the map is ergodic and mixing. The exponential growth of the number of periodic orbits is determined by the topological entropy which is also $\ln 2$. The enumeration of periodic orbits and their structure plays a crucial role in the semiquantum operator as well. Let

$$\nu = \sum_{k=0}^{t-1} a_k 2^k, \quad \text{and} \quad \overline{\nu} = \sum_{k=0}^{t-1} a_k 2^{t-k-1} \tag{7}$$

be the binary expansion of an integer $\nu\,(0 \leqslant \nu \leqslant 2^t - 1)$ and $\overline{\nu}$ is an integer whose binary expansion contains the corresponding bit-reversed string, read from right to left. The period-t points are at

$$q_\nu = \frac{\nu}{2^t - 1}, \quad p_\nu = \frac{\overline{\nu}}{2^t - 1}, \tag{8}$$

and there are 2^t of these. Thus the classical map is in many ways exactly solvable, if fully chaotic, and moreover is a caricature of what happens in the neighborhood of homoclinic intersections of stable and unstable manifolds that are the genesis of Hamiltonian chaos [24].

B. Quantum map

The quantization is complicated by the lack of a Hamiltonian, even a time-dependent one, such as exists for the standard map or the kicked top, other well studied models of low-dimensional chaos. Nevertheless Balazs and Voros observed that the generating function of the transformation from the left half L to the bottom half B is $F_2(q, P) = 2qP$. From the correspondence of the unitary propagator being the exponential of the classical generating function, the *mixed* representation of the transformation of $L \mapsto B$ is $\langle P|B|q\rangle \sim e^{-i2qP/\hbar}$. As the phase space is now a compact torus, the quantization is also one which takes this into account and subsequently the Hilbert space is a finite one, its dimension $N = A/h$, where A is the area of the torus, which we take as 1. Hence $h = 1/N$ is the effective Planck constant and the position states labeled by $|n\rangle$, $0 \leqslant n \leqslant N - 1$ are related to

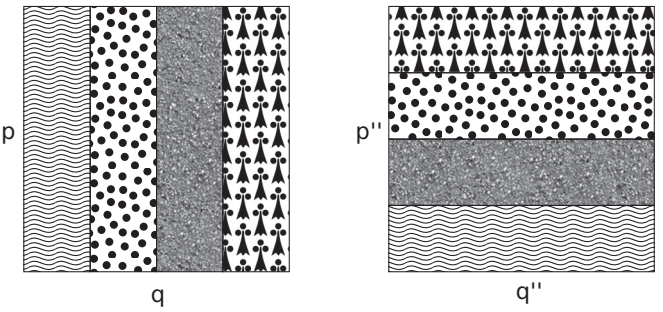

FIG. 2. Action on the unit-square phase space of the bakers map iterated twice. The four identical vertical rectangles are each stretched and compressed by a factor of 4 into corresponding horizontal rectangular partitions. Notice that unlike in Fig. 1 the patterns in the partitions are not faithfully stretched or compressed in this illustration.

the momentum states via the discrete Fourier transform. Thus the quantization of the bakers map was proposed to be the unitary operator, written in position basis to be

$$B = G_N^{-1}\begin{pmatrix} G_{N/2} & 0 \\ 0 & G_{N/2} \end{pmatrix}, \tag{9}$$

where

$$\langle m|G_N|n\rangle = \frac{1}{\sqrt{N}} \exp\left[-\frac{2\pi i}{N}(m + 1/2)(n + 1/2)\right] \tag{10}$$

is the discrete Fourier transform. The shifts by $1/2$ were added by Saraceno to restore parity symmetry, which also enabled a detailed study of eigenstates and time-evolving coherent states in the quantum baker [44]. The $R \mapsto T$ part of the transformation is the lower block $G_{N/2}$. The factor of $1/2$ in the Fourier transforms originates from the stretching of the classical baker being by the factor 2. Thus propagation of states by the bakers maps are given by $B^t|\phi_0\rangle$ and operators evolves as $B^{-t}A(0)B^t$, with t being integers, but there are no simple forms for the powers B^t, a fact related to the lack of analytical understanding of the spectra.

The time t *semiquantum* propagator B_t is constructed by quantizing the classical baker iterated t times [32]. This is unique to the baker map, and $B^t \neq B_t$, but it is believed that $B_t \approx B^t$ until the time that B_t can be defined which is at most the Ehrenfest time of $\log_2 N$. When $N = N_0 2^T$, where N_0 is an odd integer, it is defined until time T and hence is the longest when N is a power of 2. For example B_2 is got on quantizing $\mathcal{T}^2$, whose action on the unit square is shown in Fig. 2. This takes the four vertical partitions of width $1/4$ to corresponding horizontal partitions of height $1/4$. Each of them can be quantized by the action of $G_{N/4}$ in the mixed representation. The position of the resulting four blocks is dictated by the period 2 orbits which are the intersections of the vertical and corresponding horizontal partitions: (00.00,01.01,10.10,11.11). In general the operator B_t is governed by the 2^t fixed points of the classical time t map (or equivalently the period-t points of the classical map). With these definitions

$$B_t = G_N^{-1}(\mathcal{I}_t \otimes G_{N/2^t}), \tag{11}$$

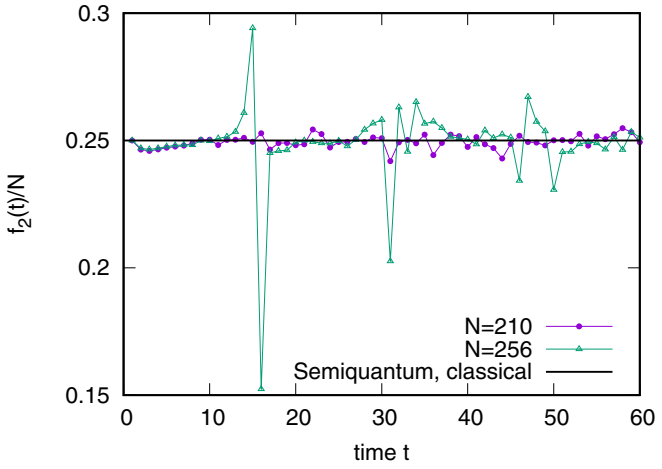

FIG. 3. The two-time correlator $f_2(t)$ in Eq. (3) is shown as a function of time for two values of N. Both reach values close to $N/4$, while the case when N is a power of 2 shows anomalous oscillations after the log time which is ≈ 8.

where $\mathcal{I}_t$ is a $2^t \times 2^t$ matrix whose entries are zero except elements $(\mathcal{I}_t)_{\nu,\bar{\nu}} = 1$, where ν and $\bar{\nu}$ are given as in Eq. (7) which determine the classical periodic orbits. For the special case of $t = 1$, $\mathcal{I}_1$ is the diagonal 2×2 identity matrix and one gets that $B_1 = B$. At $t = 2$, the $(\nu, \bar{\nu})$ pairs are (0,0),(1,2),(2,1),(3,3) and $\mathcal{I}_2$ is a "two-qubit swap gate," hence

$$B_2 = G_N^{-1} \begin{pmatrix} G_{N/4} & 0 & 0 & 0 \\ 0 & 0 & G_{N/4} & 0 \\ 0 & G_{N/4} & 0 & 0 \\ 0 & 0 & 0 & G_{N/4} \end{pmatrix}. \tag{12}$$

If $N = 2^T$, B_T will in the mixed representation (the second matrix) consist of 2^T c numbers; beyond that this is not defined—the classical partitions have reached the size of $\hbar$. This is also the "log time" or the Ehrenfest time $t_{EF} = \ln(1/h)/\lambda = \log_2 N$, beyond which even initially maximally localized states suffer interference.

III. OUT-OF-TIME-ORDERED CORRELATOR

The operator we choose is the projector $P(0) = \sum_{n=j_{\min}}^{j_{\max}} |n\rangle\langle n|$, where $|n\rangle$ are position eigenstates, and which has a clear classical limit. If $j_{\min} = 0$ and $j_{\max} = N/2 - 1$ it is the characteristic function of the left half vertical partition, the rectangle L shown in Fig. 1, The quantity of interest is

$$f(t) = -\tfrac{1}{2}[P(0), P(t)]^2 = \|\tilde{B}^t\|^2 - \|\tilde{B}^{\dagger t}\tilde{B}^t\|^2, \tag{13}$$

where $\tilde{B}^t$ is the J dimensional truncation of B^t. Figure 3 displays a normalized correlator $f_2(t)/N$ for the case when $j_{\min} = 0$ and $j_{\max} = N/2 - 1$ for two cases of $N = 210$ and $N = 256$. The former case shows small fluctuations around $1/4$, while for the latter there are large fluctuations observed at $2\log_2 N$, twice the log time, and possibly multiples of these with decreasing amplitude. Note that $f_2(0) = N/2$, thus there is an instantaneous change to values close to $N/4$ for $t > 0$. This reflects the immediate mixing of the L partition, in the sense that the classical characteristic function spreads so that $1/2$ of it is always in L for all subsequent times. To control the rate of mixing, coupled bakers maps were studied with tunable coupling in [37] whose quantum versions were studied [36]. See also [45] for such systems on a spherical phase space. The large fluctuations in $f_2(t)$ when N is a power of 2, especially at twice the log time, is consistent with known eccentricities of the quantum baker. This results in strongly localized eigenstates that are in fact all multifractal. Approximate subsets of eigenstates can be in this case constructed based on the ubiquitous, self-similar, binary Thue-Morse sequence and its generalizations [46]. However these eccentricities are prominent only at times beyond the log time and therefore for the present purpose they do not really concern us; for example the two cases of N in Fig. 3 are essentially the same before the log time.

A. Two-point correlator

While we cannot compute analytically $f_2(t) = \|\tilde{B}^t\|^2$ even for the bakers map above, the semiquantum $f_{2SQ}(t) = \|\tilde{B}_t\|^2$ turns out to be exactly $N/4$ for $t > 0$ and hence is completely consistent with the classical. To begin we write B_t in the mixed (momentum-position) basis and denote momentum states as $|\tilde{m}\rangle$. This is the matrix $\mathcal{I}_t \otimes G_{N/2^t}$, but it helps to write it explicitly as

$$\langle\tilde{m}|B_t|n\rangle = \sqrt{\frac{2^t}{N}} \exp\left[\frac{-2^{t+1}\pi i}{N}\left(m + \frac{1}{2} - \frac{\nu N}{2^t}\right)\left(n + \frac{1}{2} - \frac{\bar{\nu} N}{2^t}\right)\right]\Theta_{m\nu}\Theta_{n\bar{\nu}}. \tag{14}$$

For any (m, n) pair (m and n take values in $[0, N-1]$) there exists a unique ν and hence $\bar{\nu}$ as $\mathcal{I}_t$ is a permutation matrix. The connection is explicit in the function $\Theta_{m\nu}$ which is $= 1$ if $\nu N/2^t \leqslant m \leqslant (\nu+1)N/2^t - 1$ and 0 otherwise. Multiplying by G_N^{-1} on the left of the above mixed representation results in the matrix element of B_t in the position basis:

$$\langle k|B_t|n\rangle = \frac{2^{t/2}}{N} e^{i\pi\bar{\nu}} \exp\left[\frac{2\pi i \nu}{2^t}\left(k + \frac{1}{2}\right)\right]\Theta_{n\bar{\nu}} \sum_{m=0}^{N/2^t-1} \exp\left\{\frac{2\pi i}{N}\left(m + \frac{1}{2}\right)\left[k + \frac{1}{2} - 2^t\left(n + \frac{1}{2}\right)\right]\right\}, \tag{15}$$

and it is convenient to keep this form without performing the geometric sum. For

$$f_{2SQ}(t) = \|\tilde{B}_t\|^2 = \sum_{k,n=0}^{N/2-1} |\langle k|B_t|n\rangle|^2 = \frac{2^t}{N^2} \sum_{k,n=0}^{N/2-1} \left| \sum_{m=0}^{N/2^t-1} \exp\left\{\frac{2\pi i}{N}\left(m + \frac{1}{2}\right)\left[k + \frac{1}{2} - 2^t\left(n + \frac{1}{2}\right)\right]\right\}\right|^2 = \frac{N}{4}, \tag{16}$$

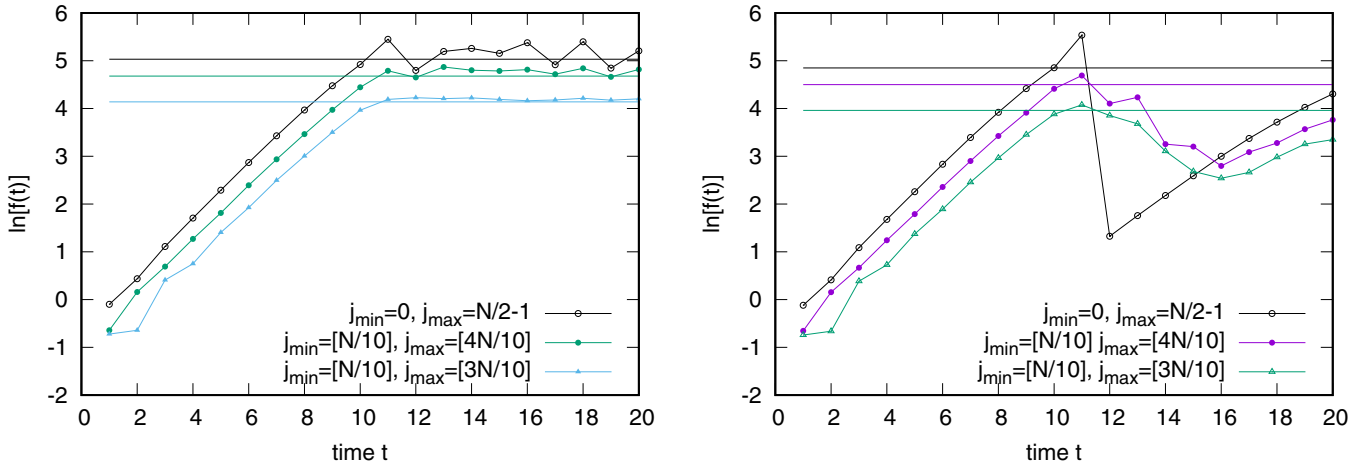

FIG. 4. The growth of the commutator's norm $f(t)$ in Eq. (5) for two values of N and for three projectors. On the left is the case with $N = 2446$ and the right has $N = 2048$. The three projectors are as in Eq. (2) with the $j_{\min}$ and $j_{\max}$ values indicated in the figure. The horizontal lines are from the random matrix saturation value in Eq. (34).

the last equality follows on performing the k and n sums first. Note that this also reflects the subunitarity of $\tilde{B}_t$ as the norm decreases from $N/2$ at $t = 0$ to $N/4$ for all $t > 0$.

B. OTOC

We now turn to the central quantity $f(t)$ which measures the noncommutativity of $P(0)$ and $P(t)$ as in Eq. (13). Figure 4 shows the growth of $f(t)$ for two different values of N and three different position space projectors $P(0)$; one is the L partition that includes the origin which is a fixed point in the classical limit $j_{\min} = 0$ and $j_{\max} = N/2 - 1$, one that excludes the origin but is still in the L partition with $j_{\min} = [N/10]$, $j_{\max} = [4N/10]$, and a third one that is in L but does not include either the origin which is a fixed point or the period-2 orbit at $(1/3, 2/3)$. It is observed that the choice of the projector does not make a difference to the growth which is close to being exponential, but the saturation that depends on the size J of the projector and has lesser fluctuations when the partition excludes low-order periodic orbits. The choice of $N = 2446$, which is such that $N/2$ is a prime number, ensures that we are far from nongeneric features, while with $N = 2048 = 2^{11}$ an extreme nongeneric case is shown. It is noted that the different partitions have now a more dramatic effect on the $f(t)$, but in fact before the log time the two cases of N and the three partition choices display differences too small to be seen in the figure. It is this growth phase that is also accessible via the semiquantum propagator B_t in Eq. (12).

We turn to an analytical derivation that is based on B_t and find the semiquantum approximation of $f(t)$ as

$$f_{SQ}(t) = \|\tilde{B}_t\|^2 - \|\tilde{B}_t^\dagger \tilde{B}_t\|^2. \tag{17}$$

Using the position representation of B_t as given in Eq. (15), and considering the projector with $j_{\min} = 0$ and $j_{\max} = N/2 - 1$ for simplicity results on further simplifications in

$$f_{SQ}(t) = \frac{1}{N^2} \sum_{k=0}^{N/2-1} \sum_{\bar{k}=N/2}^{N-1} \left| \sum_{\bar{\nu}=0}^{2^{t-1}-1} \exp\left[\frac{2\pi i}{2^t} \nu(k-\bar{k})\right] \right|^2 \left| \sum_{m=0}^{N/2^t-1} \exp\left[\frac{2\pi i}{N} m(k-\bar{k})\right] \right|^2. \tag{18}$$

Note that the third sum is over $\bar{\nu}$ but the argument contains the complementary ν. Further simplifications are indeed possible. First we have

$$\left| \sum_{m=0}^{N/2^t-1} \exp\left[\frac{2\pi i}{N} ml\right] \right|^2 = \frac{\sin^2(\pi l/2^t)}{\sin^2(\pi l/N)}. \tag{19}$$

Then we notice that the $\bar{\nu} < 2^{t-1}$ condition implies that the most significant bit of the momentum is 0, that is the periodic orbit, corresponding to the block ν below $p = 1/2$. Therefore the string ν has the least significant bit to be 0, the rest being arbitrary. This just implies that ν is any even integer from $\{0, 2, \ldots, 2^t - 2\}$, say $2n$. Then

$$\sum_{\bar{\nu}=0}^{2^{t-1}-1} \exp\left[\frac{2\pi i}{2^t} \nu(k-\bar{k})\right] = \sum_{n=0}^{2^{t-1}-1} \exp[2\pi i n(k-\bar{k})/2^{t-1}] = 2^{t-1}\delta[(\bar{k}-k) \equiv 0 \bmod 2^{t-1}], \tag{20}$$

and the semiquantum OTOC reduces to

$$f_{SQ}(t) = \frac{2^{2t-2}}{N^2} \sum_{k=0}^{N/2-1} \sum_{\bar{k}=N/2}^{N-1} \delta[(\bar{k}-k) \equiv 0 \bmod 2^{t-1}] \frac{\sin^2(\pi(k-\bar{k})/2^t)}{\sin^2(\pi(k-\bar{k})/N)}. \tag{21}$$

Due to the Kronecker delta and the numerator in the $\sin^2$ terms only those pairs of $(k, \bar{k})$ will contribute whose difference $(\bar{k}-k)$ is an *odd multiple of* 2^{t-1}.

Let $N = 2^T N_0$ where N_0 is an odd number $\geqslant 1$ and $T \geqslant 1$. The semiquantum propagator B_t is strictly defined for times $t \leqslant T$. The double sum in Eq. (21) can be reduced further as the argument depends only on the difference $l = (\bar{k}-k)$ which can take values in $[1, N-1]$. Let the number of $(\bar{k}, k)$ pairs that give the same l value be d_l. Then

$$d_l = \begin{cases} l & 1 \leqslant l \leqslant N/2 \\ N-l & N/2 < l \leqslant N-1. \end{cases} \tag{22}$$

Therefore

$$f_{SQ}(t) = \frac{2^{2t-2}}{N^2} \sum_{l=1}^{N-1} d_l \, \delta[l \equiv 0 \bmod 2^{t-1}] \frac{\sin^2(\pi l/2^t)}{\sin^2(\pi l/N)}. \tag{23}$$

As both d_l and the other quantities being summed over share the symmetry $l \to N-l$, it follows that

$$f_{SQ}(t) = \frac{2^{2t-2}}{N^2} \left[2 \sum_{l=1}^{N/2-1} l \, \delta[l \equiv 0 \bmod 2^{t-1}] \frac{\sin^2(\pi l/2^t)}{\sin^2(\pi l/N)} + \frac{N}{2} \sin^2(\pi N_0 2^{T-t-1}) \right]. \tag{24}$$

Thus whenever $1 \leqslant t \leqslant T-1$ the last term within the brackets, corresponding to $l = N/2$, vanishes.

Assuming that this is the case, we get on setting $l = (2k+1)2^{t-1}$ the restriction $k = 0, 1, \ldots, 2^{T-t-1}-1$, and hence for $1 \leqslant t \leqslant T-1$

$$f_{SQ}(t) = \frac{2^t}{16\, M^2} \sum_{k=0}^{M-1} \frac{2k+1}{\sin^2\left[\frac{\pi(2k+1)}{4M}\right]} \tag{25}$$

with $M = 2^{T-t-1} N_0 = N/2^{t+1}$.

In fact for N powers of 2, $N_0 = 1$ and the following are easily seen to be true:

$$f_{SQ}(t = T-2) = \left(2 - \frac{1}{\sqrt{2}}\right) 2^{T-5},$$
$$f_{SQ}(t = T-1) = 2^{T-4}, \quad f_{SQ}(t = T) = 2^{T-3}. \tag{26}$$

Figure 5 compares this semiquantum evaluation with the quantum one for $f(t)$ when $N = 1024$. It works well enough that visible differences are very small. It is also seen to work well for generic dimensions such as $N = 2446$, where $M = [N/2^{t+1}]$ is used in Eq. (25). We may conclude that the Lyapunov exponent based on the OTOC is $\ln 2$, except that there is a weak dependence of time in the coefficient of 2^t in Eq. (25). To evaluate the coefficient, the sum has to be performed, and for large M, it may be replaced by an integral, but this diverges and the singularity at $k = 0$ must be compensated by adding and subtracting an appropriate sum to remove the singularity from the integral,

$$\frac{1}{M^2} \sum_{k=0}^{M-1} \frac{2k+1}{\sin^2\left[\frac{\pi(2k+1)}{4M}\right]}$$
$$\approx \frac{1}{2} \int_0^2 \frac{x\, dx}{\sin^2(\pi x/4)} - 8 \int_0^2 \frac{x\, dx}{\pi^2 x^2} + \frac{16}{\pi^2} \sum_{k=0}^{M-1} \frac{1}{2k+1}$$
$$= \frac{8}{\pi^2}[1 + \ln(8/\pi) + \gamma + \psi_0(M+1/2)]$$
$$= \frac{8}{\pi^2}[1 + \ln(8/\pi) + \gamma + \ln M + O(1/M^2)], \tag{27}$$

where $\psi_0(x)$ is the digamma function and γ the Euler constant. Finally then an approximate form of $f_{SQ}(t)$ is

$$f_{SQ}(t) = \frac{2^t}{2\pi^2} \left[\ln\left(\frac{4\, e^{\gamma+1}}{\pi} \frac{N}{2^t}\right) + O(2^{t+1}/N)^2 \right]. \tag{28}$$

This is valid when $N = N_0 2^T$, $1 \leqslant t \leqslant T-1$, and $M = N/2^{t+1} \gg 1$, that is for times much smaller than the log time. In practice it appears to be a good approximation almost close to the log time. The $\hbar \to 0$ (here $N \to \infty$) and $t \to \infty$ limits cannot be interchanged. Based on the above expression, the following holds:

$$\lim_{t\to\infty} \frac{1}{t} \ln f_{SQ}(t) = \ln 2, \tag{29}$$

if $N = N_0 2^{t+t_0}$, where $t_0 > 1$ and $N_0 \geqslant 1$ are constants. That is in this limit, the long time limit is slaved to $\hbar \to 0$. If we want the time t to be fixed, the following is true for

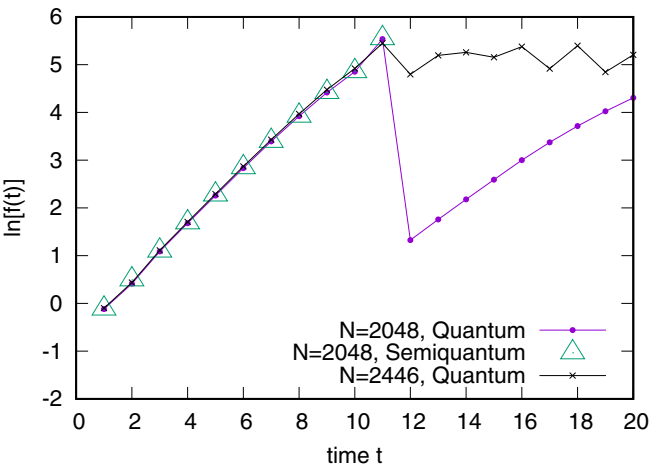

FIG. 5. Comparison of the semiquantum analytical evaluation in Eq. (25) with the quantum growth of $f(t)$.

instantaneous rates:

$$\frac{f_{SQ}(t+1)}{f_{SQ}(t)} \approx 2\left[1 - \frac{\ln 2}{\ln(N_0 2^{T-t-1})}\right] \to 2 \qquad (30)$$

as $N_0 \to \infty$. Thus the rate also approaches 2 classically, but very (logarithmically) slowly. The above expressions are consistent then with

$$f(t) \approx f_{SQ}(t) \sim C_1 e^{\lambda t} \ln\left(\frac{C_2}{e^{\lambda t}\hbar}\right), \quad t < t_{EF} = \ln(1/\hbar)/\lambda, \qquad (31)$$

where $\lambda = \ln 2$ is the classical Lyapunov exponent of the baker map, and C_1, C_2 are positive constants.

The operators used in this paper are projectors and hence they have no smooth classical limit. We have verified numerically that using operators such as $\cos(2\pi q)$ also lead to the same growth of $f(t)$, namely $\approx 2^t$. Work with smooth maps such as the standard map shows that the rate is approximately twice the classical Lyapunov exponent when operators with smooth classical limits are employed. That the rate of the growth of OTOC in the quantum bakers map, as found above, is only $\lambda = \ln 2$ rather than $2 \ln 2$ is therefore worth emphasizing. The main source of the baker's eccentricities lie in its discontinuous nature. This begs the question if other discontinuous systems share such features. It also seems to contradict the expectation that quantum diffraction effects will lead to enhancing the chaos, rather than suppressing it.

At the instigation of a referee the quantum sawtooth map [47], which is a discontinuous map, was studied as well. While we do not present details here, the results are consistent with the fact that the growth of OTOCs, before the Ehrenfest time, in such systems is exponential with a rate that is closer to λ rather than 2λ. Interestingly the sawtooth map as a special case has the smooth cat maps for which indeed the growth occurs at the rate of 2λ (consistent with [9]). However the diffractive cases do have an initially large OTOC that outstrips the smooth cases to compensate for the subsequent slower growth, to allow for the same saturation value at the Ehrenfest times. The exact time scales at which the slower growth rate starts needs further study, but seems to be part of a "diffusive," possibly operator dependent, regime $< t_d$. Thus the quantum baker is not alone in having the slower growth rate, but more detailed investigations are left for the future.

C. Saturation value

Beyond the log time, $f(t)$ or the OTOC saturates and in the bakers map it appears that there is no real gap between the two. The saturation value follows if we assume that U^t is chosen from a random set of uniformly distributed unitary matrices of dimension N, namely the standard circular unitary ensemble (CUE) of random matrix theory (RMT). While a general result in terms of any operator can be given, we focus on the projection operator as in Eq. (2) treated above and use the first equality of Eq. (5) to write

$$f(t) = \sum_{j,j',j'' \in J} \sum_{\bar{j} \in \bar{J}} U_{jj'} U^*_{\bar{j}j'} U_{\bar{j}j''} U^*_{jj''}, \qquad (32)$$

where we simply write U for U^t and now treat U as a member of the CUE and average over the ensemble. Using

$$\begin{aligned}\langle U_{i_1 j_1} U_{i_2 j_2} U^*_{i'_1 j'_1} U^*_{i'_2 j'_2} \rangle_{\mathrm{CUE}} &= \frac{1}{N^2-1}(\delta_{i_1 i'_1}\delta_{i_2 i'_2}\delta_{j_1,j'_1}\delta_{j_2 j'_2} + \delta_{i_1 i'_2}\delta_{i_2,i'_1}\delta_{j_1 j'_2}\delta_{j_2 j'_1}) \\ &\quad - \frac{1}{N(N^2-1)}(\delta_{i_1 i'_1}\delta_{i_2 i'_2}\delta_{j_1,j'_2}\delta_{j_2 j'_1} + \delta_{i_1 i'_2}\delta_{i_2,i'_1}\delta_{j_1 j'_1}\delta_{j_2 j'_2}),\end{aligned} \qquad (33)$$

we get

$$\langle f(t) \rangle_{\mathrm{CUE}} = \frac{J^2(N-J)^2}{N(N^2-1)}. \qquad (34)$$

For the case when $J = N/2$ we get $\langle f(t) \rangle_{\mathrm{CUE}} = N/16$ for large N. It is remarkable that the semiquantum evaluation in Eq. (26) gives $f(T-1) = N/16$ as well and hence when N is a power of 2, the semiquantum OTOC matches exactly the RMT value at which saturation occurs. The value at $t = T$ is anomalously higher, a feature that seems to hold for all values of N. Figure 4 shows the RMT value for different partition sizes J and one sees reasonable agreement. Thus for the bakers map, the semiquantum approximation, along with the RMT saturation value, gives a complete picture of the OTOC or the commutator growth $f(t)$.

IV. DISCUSSIONS

The quantization of the bakers map presents an almost exactly solvable model of quantum chaos as far as the OTOC is concerned. The semiquantum approximation is crucial in making this possible and indicates that along with the exponential growth there is also an additional linear time dependence that grows into prominence at the log time. While the explicit analytical evaluation in Eq. (25) is for partitions that include the origin, the additional time dependence also persists if it does not. It is clear that there cannot be a pure exponential growth as it has to give way to a post-log-time growth that eventually saturates to the RMT value. Whether the form in, say, Eq. (28) can be generic remains to be seen. Due to the discontinuities in the bakers map, it is known to have anomalous features such as additional $\ln N$ terms in semiclassical trace formulas [32,48]. It is possible that these also contribute anomalously to the OTOC. Yet, the exact nature of the time dependence of the OTOC including an exponential behavior and saturation to a RMT value are generic features. The N values that are powers of 2 are also special and have multifractal states and nongeneric features, however these only dominate the post-log-time phase, when instead of saturating they display oscillations.

Finally as noted in this paper, the truncations of powers of the quantum map determined the OTOCs and in fact have more information in them. While the OTOC is determined by the singular values, it is also of interest to study the eigenvalues. Figure 6 shows the eigenvalues for the first 16 times when $N = 1024$ for the truncation with $j_{\min} = 0$ and $j_{\max} = N/2 - 1$. It is seen that to begin with a majority of the eigenvalues are very small, and that within the log-time period they increase and predominantly occupy the area within the

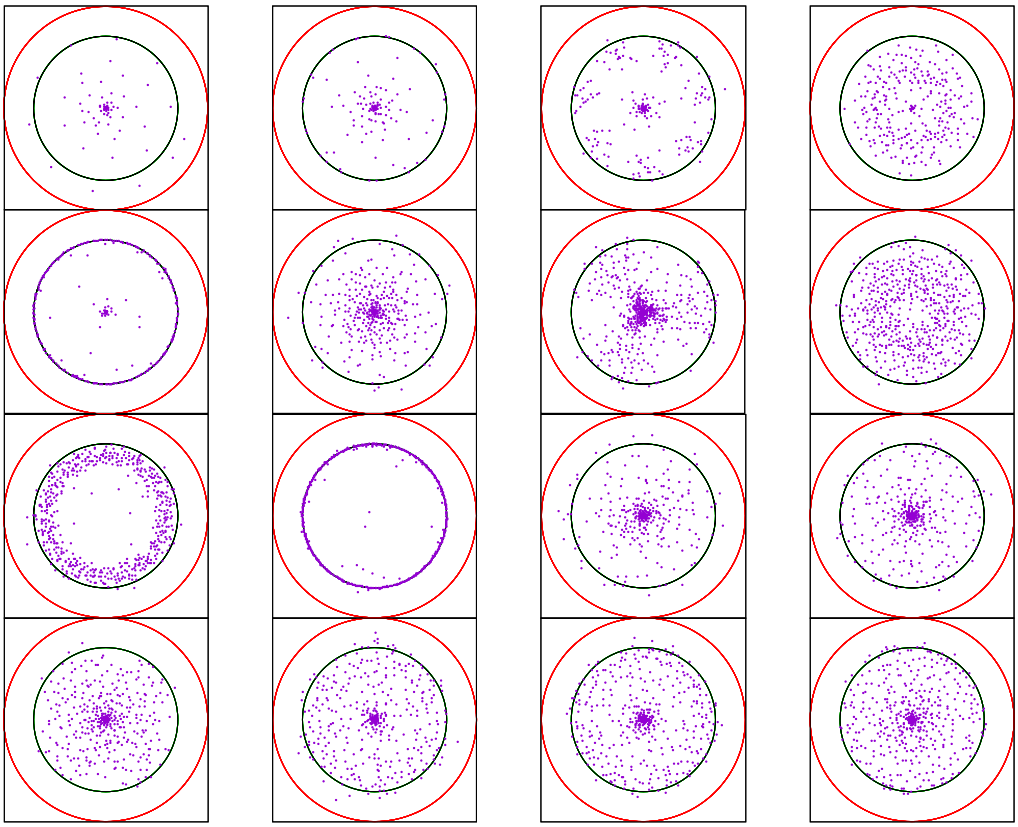

FIG. 6. The eigenvalues of the $N/2 \times N/2$: left-top corner truncation of B^t, that is $\tilde{B}^t$, for $t = 1$ to 16 and $N = 1024$. The time increases from left to right and top to bottom. shown are the real and imaginary parts of the eigenvalues, as well as the unit circle and the circle with radius $1/\sqrt{2}$ are shown.

circle of radius $1/\sqrt{2}$. Random unitary matrices with such truncations are known to have eigenvalues whose modulus is less that $1/\sqrt{2}$ [49] and hence this reflects the way in which the powers of the bakers map randomizes. It is a peculiarity of the bakers map at N powers of 2 that the eigenvalues have curious structures at specific times. Notably at $t = \log_2 N$ it lies almost wholly on the circle with radius $1/\sqrt{2}$ and subsequently again "collapses" with many eigenvalues being small once more. This is consistent with the behavior of $f(t)$ just past the log time for such powers of 2 dimensionality.

Recent work [9] has also highlighted an exact evaluation of the OTOC in the quantum cat map and this grows as $e^{2\lambda t}$ just as in the standard map [6]. Additionally the regime beyond the log time was studied from the point of view of Ruelle-Pollicott resonances. The present work indicates that the growth of the norm of truncated Perron-Frobenius operators, via its singular values, may well reflect the quantum OTOC growth. It maybe noted that the spectrum of such truncated operators has already been studied in the literature [50], but that our discussion above provides an impetus for exploring more closely the role of the Perron-Frobenius operator in the growth of the OTOC. While this paper did not discuss operator scrambling, which does not occur in the (unperturbed) quantum cat map, the bakers map's scrambling ability is also accessible via the semiquantum operator and is part of future work.

ACKNOWLEDGMENTS

I am grateful to S. Ganeshan, E. B. Rozenbaum, and V. Galitzki for discussions regarding OTOCs at an early stage of this work.

[1] M. C. Gutzwiller, *Chaos in Classical and Quantum Mechanics* (Springer-Verlag, New York, 1990).

[2] F. Haake, *Quantum Signatures of Chaos* (Spring-Verlag, Berlin, 1991).

[3] L. Reichl, *The Transition to Chaos: In Conservative Classical Systems: Quantum Manifestations*, Institute for Nonlinear Science (Springer, New York, 2013).

[4] A. M. Ozorio de Almeida, *Hamiltonian Systems: Chaos and Quantization*, Cambridge Monographs on Mathematical Physics (Cambridge University Press, Cambridge, UK, 1989).

[5] *Chaos et Physique Quantique/Chaos and Quantum Physics*, Proceedings of Les Houches Summer School, Session LII, edited by M. J. Giannoni, A. Voros, and J. Zinn-Justin (North-Holland, Amsterdam, 1991).

[6] E. B. Rozenbaum, S. Ganeshan, and V. Galitski, Lyapunov Exponent and Out-of-Time-Ordered Correlator's Growth Rate in a Chaotic System, Phys. Rev. Lett. **118**, 086801 (2017).

[7] K. Hashimoto, K. Murata, and R. Yoshii, Out-of-time-order correlators in quantum mechanics, J. High Energy Phys. 10 (2017) 138.

[8] R. A. Jalabert, I. García-Mata, and D. A. Wisniacki, Semiclassical theory of out-of-time-order correlators for low-dimensional classically chaotic systems, Phys. Rev. E **98**, 062218 (2018).

[9] I. García-Mata, M. Saraceno, R. A. Jalabert, A. J. Roncaglia, and D. A. Wisniacki, Chaos Signatures in the Short and Long Time Behavior of the Out-of-Time Ordered Correlator, Phys. Rev. Lett. **121**, 210601 (2018).

[10] X. Chen and T. Zhou, Operator scrambling and quantum chaos, arXiv:1804.08655.

[11] J. S. Cotler, D. Ding, and G. R. Penington, Out-of-time-order operators and the butterfly effect, Ann. Phys. **396**, 318 (2018).

[12] A. Seshadri, V. Madhok, and A. Lakshminarayan, Tripartite mutual information, entanglement, and scrambling in permutation symmetric systems with an application to quantum chaos, Phys. Rev. E **98**, 052205 (2018).

[13] S. Moudgalya, T. Devakul, C. W. von Keyserlingk, and S. L. Sondhi, Operator spreading in quantum maps, arXiv:1808.04889.

[14] J. Maldacena, S. H. Shenker, and D. Stanford, A bound on chaos, J. High Energy Phys. 08 (2016) 106.

[15] N. Lashkari, D. Stanford, M. Hastings, T. Osborne, and P. Hayden, Towards the fast scrambling conjecture, J. High Energy Phys. 04 (2013) 022.

[16] D. A. Roberts and B. Swingle, Lieb-Robinson Bound and the Butterfly Effect in Quantum Field Theories, Phys. Rev. Lett. **117**, 091602 (2016).

[17] S. H. Shenker and D. Stanford, Black holes and the butterfly effect, J. High Energy Phys. 03 (2014) 067.

[18] M. Berry, N. Balazs, M. Tabor, and A. Voros, Quantum maps, Ann. Phys. **122**, 26 (1979).

[19] F. M. Izrailev, Simple models of quantum chaos: Spectrum and eigenfunctions, Phys. Rep. **196**, 299 (1990).

[20] V. I. Arnol'd and A. Avez, *Ergodic Problems of Classical Mechanics* (Benjamin, New York, 1968).

[21] J. Hannay and M. Berry, Quantization of linear maps on a torus-Fresnel diffraction by a periodic grating, Physica D (Amsterdam) **1**, 267 (1980).

[22] E. Hopf, *Ergodentheorie* (Springer-Verlag, Berlin, 1937).

[23] S. Strogatz, *Nonlinear Dynamics and Chaos* (CRC, Boca Raton, 2015).

[24] E. Ott, *Chaos in Dynamical Systems*, 2nd ed. (Cambridge University Press, Cambridge, UK, 2002).

[25] D. S. Ornstein, Ergodic Theory, Randomness, and "Chaos", Science **243**, 182 (1989).

[26] N. L. Balazs and A. Voros, The Quantized Baker's Transformation, Europhys. Lett. **4**, 1089 (1987).

[27] N. L. Balazs and A. Voros, The quantized Baker's transformation, Ann. Phys. **190**, 1 (1989).

[28] T. A. Brun and R. Schack, Realizing the quantum baker's map on a NMR quantum computer, Phys. Rev. A **59**, 2649 (1999).

[29] Y. S. Weinstein, S. Lloyd, J. Emerson, and D. G. Cory, Experimental Implementation of the Quantum Baker's Map, Phys. Rev. Lett. **89**, 157902 (2002).

[30] A. J. Scott and C. M. Caves, Entangling power of the quantum baker's map, J. Phys. A **36**, 9553 (2003).

[31] M. L. Mehta, *Random Matrices* (Elsevier, New York, 2004), Vol. 142.

[32] M. Saraceno and A. Voros, Towards a semiclassical theory of the quantum baker's map, Physica D: Nonlin. Phenom. **79**, 206 (1994).

[33] A. Lakshminarayan and N. L. Balazs, On the noncommutativity of quantization and discrete time evolution, Nucl. Phys. A **572**, 37 (1994).

[34] A. O. de Almeida and M. Saraceno, Periodic orbit theory for the quantized baker's map, Ann. Phys. **210**, 1 (1991).

[35] M. Degli Esposti, S. Nonnenmacher, and B. Winn, Quantum Variance and Ergodicity for the Baker's Map, Commun. Math. Phys. **263**, 325 (2006).

[36] A. Lakshminarayan and N. L. Balazs, Relaxation and localization in interacting quantum maps, J. Stat. Phys. **77**, 311 (1994).

[37] Y. Elskens and R. Kapral, Reversible dynamics and the macroscopic rate law for a solvable Kolmogorov system: The three bakers' reaction, J. Stat. Phys. **38**, 1027 (1985).

[38] D. Ruelle, Resonances of Chaotic Dynamical Systems, Phys. Rev. Lett. **56**, 405 (1986).

[39] K. Zyczkowski and H.-J. Sommers, Truncations of random unitary matrices, J. Phys. A **33**, 2045 (2000).

[40] Y. V. Fyodorov and H.-J. Sommers, Random matrices close to Hermitian or unitary: Overview of methods and results, J. Phys. A **36**, 3303 (2003).

[41] S. H. Simon and A. L. Moustakas, Crossover from Conserving to Lossy Transport in Circular Random-Matrix Ensembles, Phys. Rev. Lett. **96**, 136805 (2006).

[42] G. Casati, G. Maspero, and D. L. Shepelyansky, Quantum Poincaré Recurrences, Phys. Rev. Lett. **82**, 524 (1999).

[43] A. Bäcker, R. Ketzmerick, S. Löck, and L. Schilling, Regular-to-Chaotic Tunneling Rates Using a Fictitious Integrable System, Phys. Rev. Lett. **100**, 104101 (2008).

[44] M. Saraceno, Classical structures in the quantized baker transformation, Ann. Phys. **199**, 37 (1990).

[45] A. Ostruszka, C. Manderfeld, K. Życzkowski, and F. Haake, Quantization of classical maps with tunable Ruelle-Pollicott resonances, Phys. Rev. E **68**, 056201 (2003).

[46] N. Meenakshisundaram and A. Lakshminarayan, Multifractal eigenstates of quantum chaos and the Thue-Morse sequence, Phys. Rev. E **71**, 065303 (2005).

[47] A. Lakshminarayan and N. L. Balazs, On the quantum cat and sawtooth maps-Return to generic behaviour, Chaos Solitions Fractals **5**, 1169 (1995).

[48] A. Lakshminarayan, On the Quantum Baker's Map and Its Unusual Traces, Ann. Phys. **239**, 272 (1995).

[49] D. Petz and J. Réffy, Large deviation for the empirical eigenvalue density of truncated Haar unitary matrices, Probab. Theory Relat. Fields **133**, 175 (2005).

[50] J. Weber, F. Haake, P. A. Braun, C. Manderfeld, and P. Seba, Resonances of the Frobenius-Perron operator for a Hamiltonian map with a mixed phase space, J. Phys. A **34**, 7195 (2001).